

# DNS AND STRUCTURE-BASED MODELING OF ROTATED HOMOGENEOUS SHEAR FLOW

**Stavros C. Kassinos\***

Department of Mechanical and Manufacturing Engineering,  
University of Cyprus, Nicosia CY1678, Cyprus  
kassinos@ucy.ac.cy

**William C. Reynolds**

Mechanical Engineering Department,  
Stanford University, Stanford CA94305-3035, USA  
wcr@eddy.stanford.edu

## ABSTRACT

Direct numerical simulations of homogeneous turbulence being sheared in a frame rotating about the spanwise are performed for a range of values of the governing parameters. The aim is to clarify the physics of rotated shear flows and to provide a complete database for use by turbulence modelers. One of the main findings of this work is that the equilibrium value of the ratio of the production rate to the dissipation rate ( $P/\epsilon$ ) of the turbulent kinetic energy is a function of the ratio of the frame rotation rate to the mean shear rate ( $\Omega^f/S$ ). This is true even for those values of  $\Omega^f/S$  corresponding to the “*unstable regime*”, where the turbulent kinetic energy,  $k$ , and its dissipation rate,  $\epsilon$ , grow exponentially in time. This result is contrary to the predictions of the model  $\epsilon$ -equation, which in turbulence modeling provides a standard method to transport the second turbulence scale. When the  $\epsilon$ -equation is used in conjunction with the  $k$ -equation,  $P/\epsilon$  is predicted to be constant and independent of  $\Omega^f/S$  in the unstable regime. Here, we show this to be an artifact of the constant coefficients used in the model  $\epsilon$ -equation. When the large-scale enstrophy equation is used in place of the  $\epsilon$ -equation, structure-based turbulence models provide excellent predictions for all one-point statistics, including the Reynolds stresses and the variation of  $P/\epsilon$  with  $\Omega^f/S$ .

## INTRODUCTION

Homogeneous shear and straining flows in rotating frames capture the basic physics of turbomachinery flows and are good configurations for the calibration and refinement of RANS models used in CFD codes. Unfortunately there is a surprising lack of modern, high resolution, simulations of rotated shear and straining flows, and this hinders model improvement and development. Recognizing this need, we have been conducting DNS for homogeneous shear and straining flows in rotating frames as part of the ASCI program at Stanford. These DNS data will be used by modeling groups to shape and tune their models to handle rotating turbomachinery flows.

The flow configuration of primary interest corresponds to the shear of homogeneous turbulence in a frame rotating about the spanwise or streamwise direction. Turbomachinery flows also involve strain dominated regions and these

\*also affiliated with the Center for Integrated Turbulence Simulations (C.I.T.S.), Stanford University, CA94305, USA

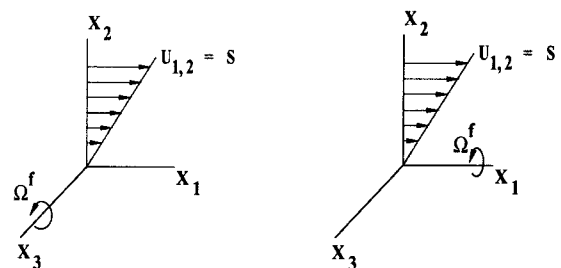


Figure 1: Flow configuration for the shear of homogeneous turbulence in a frame rotating about the spanwise direction (left) and about the streamwise direction (right).

can be emulated by straining homogeneous turbulence in a rotating frame. Simulation plans anticipate both strain and shear cases, and a single general purpose code has been built to handle all configurations.

The discussion that follows is limited to the case of shear in a frame rotating about the spanwise (see Fig. 1). Simulations for the case where the frame is rotating about the streamwise have been initiated, but will be discussed elsewhere.

## DNS: CODE IMPLEMENTATION

The numerical method used to solve the governing equations for homogeneous shear flows is similar to that introduced by Rogallo (1981). The governing equations are transformed to a set of coordinates which deform with the mean flow. This allows Fourier pseudo-spectral methods, with periodic boundary conditions, to be used for the representation of the spatial variation of the flow variables. Time advance is accomplished by a third-order Runge-Kutta method. Since the mean imposed shear skews the computational grid with time, periodic remeshing of the grid is needed in order to allow the simulation to progress to large total shear where a self-preserving regime might be expected to prevail. The periodic remeshing introduces aliasing errors that are removed by a de-aliasing procedure included in the code. An MPI based version of the code has been implemented in Vectoral and ported to the ASCI Red machine.

## STRUCTURE-BASED TURBULENCE MODELING

This modeling effort was initiated in the late 80's

Reynolds (1989) with the introduction of the idea that the Reynolds stresses, which reflect the active velocity components, by themselves do not reveal much about the turbulence structure. At the same time, we also introduced a new structure tensor describing the dimensionality of the turbulence, and suggested that this and other one-point tensors might be used in a new approach to turbulence modeling that we called “Structure-Based Modeling” (SBM). Over the past decade we have developed and refined the one-point tensor representations of turbulence structure (Kassinis, Reynolds & Rogers, 2001; Reynolds & Kassinis, 1995; Kassinis & Reynolds 1994). We have also developed a differential structure-based model that did well in modeling complex homogeneous and inhomogeneous flows, including rotating pipe flow where it was shown to perform better than other models (Poroseva, Kassinis, Langer & Reynolds, 2002). We have recently developed an algebraic modeling of the key structure tensors in terms of local mean strain and rotation rates and the turbulence time scale. We plan to use this algebraic model, along with transport equations for two appropriate turbulence scales, in a robust and widely applicable engineering model that should be useful in the design of complex rotating flow systems.

#### Summary of the structure tensors

A brief summary of our new structure tensors is presented here. For more detail see Kassinis et al. (2001) and Reynolds & Kassinis (1995). The tensors are defined using the vector stream function of the turbulence, which in turn is defined by

$$u'_i = \epsilon_{ijk} \Psi'_{k,j} \quad \Psi'_{i,kk} = -\omega'_i \quad \Psi'_{k,k} = 0. \quad (1)$$

Note that  $\Psi'$  is a local quantity that contains non-local turbulence information.

The Reynolds stress tensor can be expressed as

$$R_{ij} = \overline{u'_i u'_j} = \epsilon_{ipm} \epsilon_{jqn} \overline{\Psi'_{m,p} \Psi'_{n,q}}. \quad (2)$$

For homogeneous turbulence

$$R_{ij} = \int E_{ij}(\mathbf{k}) d^3 \mathbf{k} \quad (3)$$

where  $E_{ij}(\mathbf{k})$  is the velocity spectrum tensor. Note that if  $u'_1 = 0$  everywhere, then  $R_{11} = 0$ . We have emphasized (Kassinis et al., 2001; Kassinis & Reynolds 1994) that  $R_{ij}$  describes the *componentality* of the turbulence, but not its *dimensionality*. Two-dimensional (2D) turbulence need not be two-component (2C); it could be 1C, 2C, or 3C.

The *dimensionality* tensor is

$$D_{ij} = \overline{\Psi'_{n,i} \Psi'_{n,j}}. \quad (4)$$

Like  $R_{ij}$ ,  $D_{ij}$  is dominated by the large-scale energy-containing turbulence. If every  $\Psi'_i$  is independent of  $x_1$ , then  $D_{11} = 0$  and the turbulence is independent of  $x_1$ . For homogeneous turbulence

$$D_{ij} = \int \frac{k_i k_j}{k^2} E_{nn}(\mathbf{k}) d^3 \mathbf{k}. \quad (5)$$

We see that  $D_{ij}$  is determined by the energy distribution along rays in  $\mathbf{k}$ -space.

The *circulicity* tensor is

$$F_{ij} = \overline{\Psi'_{i,n} \Psi'_{j,n}}. \quad (6)$$

For homogeneous turbulence

$$F_{ij} = \int \frac{1}{k^2} W_{ij}(\mathbf{k}) d^3 \mathbf{k} \quad (7)$$

where  $W_{ij}(\mathbf{k})$  is the vorticity spectrum tensor. Hence  $F_{ij}$  is determined by the vorticity of the large-scale energy-containing turbulence. If the large-scale vorticity is aligned with the  $x_1$  axis, then  $F_{ij} = 0$  except for  $F_{11}$ .  $F_{ij}$  provides information on the large-scale circulation of the turbulence.

For homogeneous turbulence all three tensors contract to twice the kinetic energy:

$$R_{ii} = D_{ii} = F_{ii} = q^2 = 2\kappa. \quad (8)$$

Moreover, for homogeneous turbulence these tensors are not linearly independent; they satisfy a constitutive relationship

$$R_{ij} + D_{ij} + F_{ij} = q^2 \delta_{ij}. \quad (9)$$

It is convenient to normalize each of these tensors by its trace:

$$r_{ij} = R_{ij}/R_{kk} \quad d_{ij} = D_{ij}/D_{kk} \quad f_{ij} = F_{ij}/F_{kk}. \quad (10)$$

Anisotropy invariant maps, such as the one introduced by Lumley (1978) for the Reynolds stress, can be formed for each of the structure tensors. For examples see Kassinis & Reynolds (1994). In terms of the normalized structure tensors, the constitutive equation for homogeneous turbulence becomes

$$r_{ij} + d_{ij} + f_{ij} = \delta_{ij}. \quad (11)$$

Consideration of the above suggests that a one-point second-order turbulence model that involves only the Reynolds stress  $R_{ij}$  is missing important information, but that a model involving two of the tensors would have all of the one-point second-order information about the energy-containing eddies. This is correct for turbulence not subjected to mean or frame rotation. A striking confirmation of this is that the rapid pressure–strain-rate model of Launder, Reece, and Rodi (1975) can be deduced, *including the constant that they found empirically*, by modeling the associated fourth-rank tensor in terms of the anisotropies of  $\mathbf{r}$  and  $\mathbf{d}$ , with all constants determined by analysis; for details see Kassinis & Reynolds (1994) and Reynolds & Kassinis (1995). However, when mean or frame rotation is present, a third-rank one-point tensor (the *stropholysis*) is also very important. Kassinis et al. (2001) give its definition and discuss its role in rotating turbulence. The differential structure-based model used for the present comparison with DNS is based on these ideas. Details of the model formulation are given in Kassinis, Langer, Haire, & Reynolds (2000) and in Poroseva, Kassinis, Langer & Reynolds (2002). The model formulation described therein makes use of the standard  $\epsilon$  equation for the transport of the second turbulence scale. In the present study, the second turbulence scale is transported using the large-scale enstrophy equation described next.

#### Large-scale enstrophy equation

In structure-based turbulence modeling, an effort is made to have both transport equations for the turbulence scales

be firmly based. The kinetic energy equation provides a solid foundation for the energy scale of the turbulence, but the second scale remains a challenge. The exact equation for the energy dissipation rate is not useful because the important terms in this equation are dominated by small-scale turbulence, whereas  $\epsilon$  is determined by nonlinear interactions of large-scale turbulence. The  $\omega$  equation, used in  $k$ - $\omega$  models, is completely ad hoc and has no formal fundamental definition.

If we accept the idea that the rate of energy cascade from the large to small scales is determined by nonlinear interactions among the large-scale motions, then only the turbulence at scales larger than the start of the inertial range of the energy spectrum should contribute to the energy feeding the cascade. Using a model spectrum, we find that approximately half of the total turbulence energy is carried by these large scales, and that the dissipation rate can be expressed as  $\epsilon = \tilde{C}_\epsilon \tilde{k} \tilde{\omega}$ , where  $\tilde{k}$  and  $\tilde{\omega}$  are the kinetic energy and vorticity of this large-scale motion, or alternatively as  $\epsilon = C_\epsilon k \tilde{\omega}$ , where  $k$  is the total turbulence kinetic energy (see Reynolds, Langer & Kassinos, 2002).

The turbulence structure tensors (Kassinos et al., 2001) are dominated by large-scale motions. The circulicity (see Eq. 7) relates to the large-scale enstrophy. During this last year, we have shown that the exact large-scale enstrophy equation provides an excellent base for a model evolution equation for the large-scale enstrophy  $\tilde{\omega}^2$ . The terms in this equation are modeled in terms of the new large-scale structure tensors. The details of how this is done are given in Reynolds et al. (2002). For homogeneous high Reynolds number turbulence, the resulting model of the  $\tilde{\omega}^2$ -equation contains two constants, which can be determined entirely by analytical reference to the asymptotic structure and decay rate of the turbulence energy for unstrained turbulence in fixed and rotating frames. The resulting set of equations for high Reynolds number homogeneous turbulence is given by

$$\frac{dk}{dt} = -\chi k \tilde{\omega} - 2r_{ij} S_{ij} k \quad (12)$$

$$\frac{d\tilde{\omega}}{dt} = -(C_{\omega^2 T}^* - C_{\omega^2 P}^* \phi) \tilde{\omega}^2 + f_{ij} S_{ij} \tilde{\omega}. \quad (13)$$

Here  $\tilde{\omega}$  is the large-scale enstrophy,  $S_{ij}$  is the mean strain tensor,  $\chi = 3d_{ij} f_{ij}$ , and  $C_{\omega^2 T}^* = 3/2$  and  $C_{\omega^2 P}^* = 4/5$  are model constants determined by analysis as described above and in Reynolds et al. (2002).

We have implemented the new  $\tilde{\omega}^2$ -equation in the thoroughly tested differential structure-based model, the  $Q$ -model (Kassinos et al, 2000; Poroseva et al., 2002). We have found that using the  $\tilde{\omega}^2$ -equation as the second turbulence scale equation improved the predictions of the  $Q$ -model for several cases of deformation of homogeneous turbulence. In fact, when homogeneous turbulence is sheared in a frame with spanwise rotation, the  $Q$ -model using the  $\tilde{\omega}^2$ -equation is in excellent agreement with the results obtained from the DNS that we have been conducting as part of the ASCI program at Stanford. Examples of the performance of the  $Q$  model using the large-scale enstrophy equation (13) are discussed next.

#### PRELIMINARY RESULTS FOR SPANWISE ROTATION

From analysis and legacy simulations we know that shear flows rotated about the spanwise axis bifurcate depending on the value of the dimensionless parameter

$$\Omega^f/S, \quad (14)$$

where  $\Omega^f \equiv \Omega_{12}^f$  is the rate of frame rotation rate and  $S \equiv U_{1,2}$  is the mean shear rate. When the frame counter rotates relative to the rotation sense of the shear, and for moderate values of  $\Omega^f/S$ , the turbulent kinetic energy and dissipation rate grow exponentially in time. For large rates of frame counter-rotation, or when the frame co-rotates with the shear, the turbulence tends to be suppressed by the frame rotation. The general features of this bifurcation are now understood, but a more detailed understanding is needed for the calibration of turbulence models. The most widely used data comes from the Large-Eddy Simulation (LES) by Bardina, Ferziger & Reynolds (1983), and even though it serves to sketch the general features of the observed bifurcation, it falls short of providing important details. The effect of the strong frame rotation on the large-scale structure of the turbulence also remains an open question. We hope that results from the current DNS and modeling effort will help clarify the physics of rotated shear flows.

For example, the evolution histories of the normalized structure tensors are shown in Figure 2 for the case  $\Omega^f/S = 0.15$ , which falls within the unstable regime of exponential growth. Here the horizontal axes correspond to the dimensionless time based on the mean shear rate  $S$ . The individual components of each tensor are identified with labels inserted in

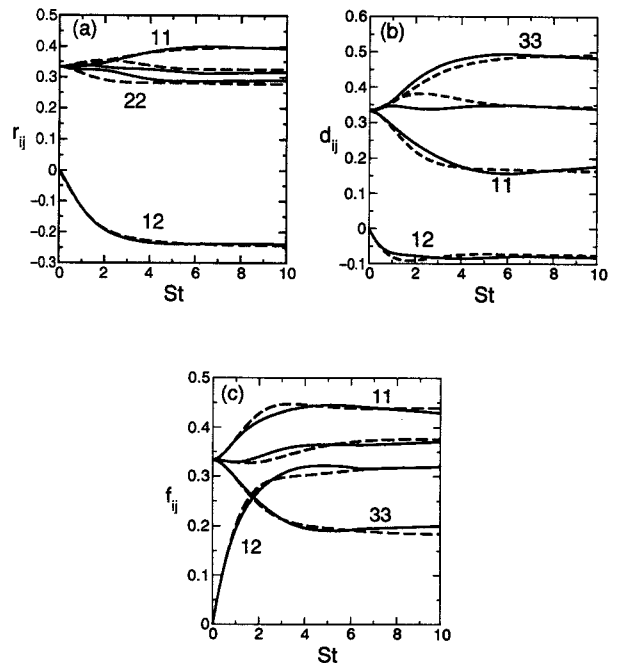


Figure 2: Evolution histories of the components of (a) the Reynolds stress tensor, (b) the dimensionality tensor and (c) the circulicity tensor. Here  $\Omega^f/S = 0.15$  and all cases were initialized with  $Sq_0^2/\epsilon_0 = 6.8$ . Tensor components are normalized by the corresponding tensor trace and are identified by labels inserted in the figure. Time is non-dimensionalized using the mean shear rate  $S$ . Shown in solid lines are the results from a  $512^3$  DNS carried out on ASCI Red, and in dashed line are the predictions of the structure-based model using the large-scale enstrophy equation.

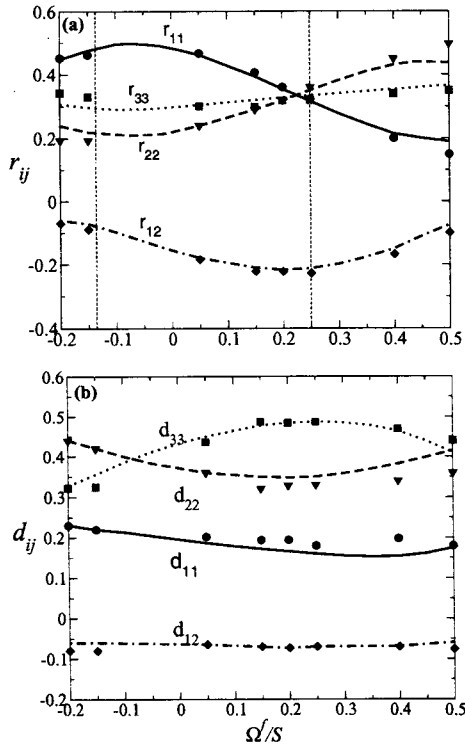


Figure 3: The components of (a) the normalized Reynolds stress tensor and (b) the normalized dimensionality tensor as function of  $\Omega^f/S$ . DNS results are shown as symbols while the predictions of the structure-based model are shown as lines: (—, ●) 11-component; (·····, ■) 22-component; (·····, ▼) 33-component; (---, ◆) 12-component.

the figure. The evolution histories obtained from the simulations (shown in solid line) are in excellent agreement with the predictions of the structure-based model using the  $\bar{\omega}^2$ -equation. This level of agreement between simulation results and model predictions are typical for all values of  $\Omega^f/S$  as can be seen by looking at the equilibrium values of the tensor components as a function of  $\Omega^f/S$  (see Fig. 3). Since the dimensionless time  $St$  at which equilibrium is first reached varies with  $\Omega^f/S$ , in Figure 3 we have chosen to compare DNS results and model predictions at  $St = 9$  for all  $\Omega^f/S$ . This value of  $St$  is large enough to ensure that at least an approximate equilibrium has been reached in all cases, and at the same time small enough to ensure that all scales of motion were in all DNS cases well resolved by the computational box. As it can be seen in Figure 3 model predictions are in excellent agreement with DNS results for the components of both  $r_{ij}$  and  $d_{ij}$ . From Eq. (11) follows that model predictions for  $f_{ij}$  must also be in good agreement with the corresponding DNS results.

In rotated shear flows, the equilibrium state depends on the ratio of the frame rotation rate  $\Omega^f \equiv \Omega_{12}^f$  to the shear rate  $S \equiv U_{1,2}$ . A limited range of values of  $\eta = \Omega^f/S$  is marked by exponential growth of both the turbulent kinetic energy,  $k$ , and the dissipation rate,  $\epsilon$ . This has been known for a while, but details of the equilibrium state of the turbulence, such as the behavior of the ratio of the turbulent kinetic energy production to dissipation rate,  $P/\epsilon$ , remained unclear. Virtually, all algebraic stress and Reynolds stress transport models using the standard  $\epsilon$  equation predict that, within this range, equilibrium turbulence is marked by  $P/\epsilon$  being

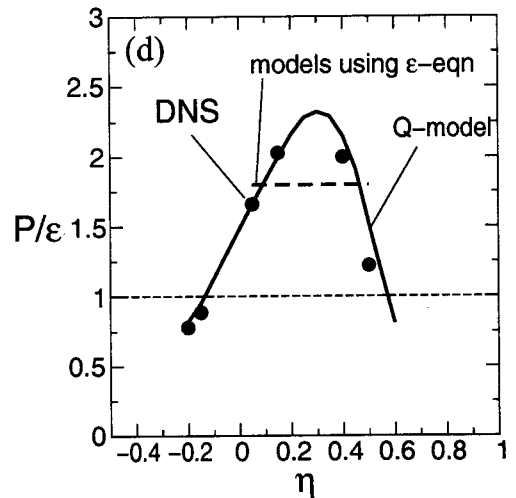


Figure 4: Equilibrium values for the of turbulent kinetic energy production to its dissipation rate  $P/\epsilon$ . DNS results are shown as symbols and the predictions of the structure-based model as a solid line. Predictions based on the standard  $\epsilon$  equations are shown in dashed line.

constant and independent of  $\eta$ . This behavior has been reported in the literature and, in the absence of DNS data that would have helped evaluate it, has been accepted as reflecting the correct physics. Preliminary results from the DNS that we are currently conducting as part of the ASCI program at Stanford show that in fact the equilibrium value of  $P/\epsilon$  is a function of  $\eta$  (see Fig. 4).

Interestingly, the  $Q$ -model using the large-scale  $\bar{\omega}^2$ -equation does predict the correct behavior for  $P/\epsilon$  with  $\eta$  (see Fig. 4), and in addition provides excellent predictions for the evolution of all normalized structure tensors in these flows (see Fig. 1). When  $\eta = \Omega^f/S$  is close to  $1/4$  the turbulent kinetic energy grows exponentially, and the energy-containing structures tend to quickly fill the computational box at which point the simulation has to be terminated. The challenge for these most unstable cases is being able to reach an equilibrium state before this occurs. To achieve this goal we will have to utilize computational grids of the order of  $1024^3$  or even bigger, as explained next.

## FUTURE PLANS

The rapid growth of the energy-containing structures in the most unstable case is reflected in the comparison of two instantaneous fields, one obtained from a weak rotation case ( $\Omega^f/S = 0.05$ ) and the other from the most unstable case ( $\Omega^f/S = 0.25$ ), as shown in Figure 5. Shown in both cases are semi-opaque, three-dimensional, iso-surfaces of velocity magnitude. These were obtained from simulations with different computational-box sizes that were thinned down to the same resolution for visualization. Both simulations were initialized with similar fields of decaying homogeneous isotropic turbulence having  $Sq_0^2/\epsilon_0 \approx 6.8$ . The field on the top was obtained at  $St = 4.6$  from a  $256^3$  preliminary simulation. In this case  $\Omega^f/S = 0.05$ , the frame rotation is weak, the turbulent kinetic energy growth is moderate, and the turbulence structures, are well contained in the computational box. In comparison, the field on the bottom was taken at  $St = 4.4$  from a  $512^3$  simulation having  $\Omega^f/S = 0.25$ . The

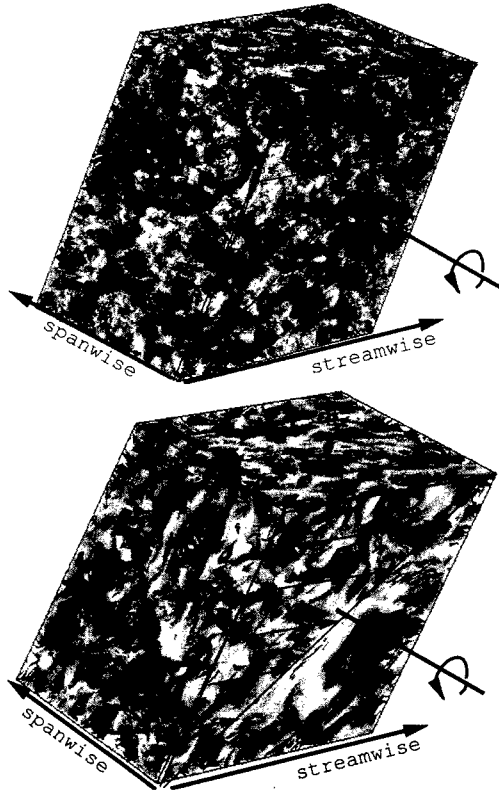


Figure 5: Velocity magnitude iso-surfaces from two simulations of homogeneous turbulence sheared in a rotating frame. Shown on the top are iso-surfaces taken at  $St = 4.6$  from a  $256^3$  simulation for the case  $\Omega^f/S = 0.05$ . Shown on the right are iso-surfaces at  $St = 4.4$  from a  $512^3$  simulation for the most unstable case  $\Omega^f/S = 0.25$ . Darker shades correspond to low and lighter shades to high velocity. The simulations were initialized with similar fields of decaying homogeneous isotropic turbulence with  $Sq_0^2/\epsilon_0 = 6.8$

level of the turbulent kinetic energy and the size of energy-containing structures are remarkably higher in this case. In fact, even at the relatively moderate total shear of  $St = 4.4$ , the  $512^3$  simulation is already close to running out of computational box.

This rapid growth of the energy-containing structure for values of  $\Omega^f/S$  in the neighborhood  $1/4$  makes it particularly difficult to reach a self-preserving (“equilibrium”) regime before larger eddies outgrow the computational box. This explains the lack of DNS data points around  $\Omega^f/S = 0.25$  in Fig. 4. We are currently carrying out a series of  $1024^3$  simulations that we expect will allow us to reach the beginning of the self-preserving regime for cases with  $\Omega^f/S$  near 0.25.

## CONCLUSION

Results from the current simulations are already providing important insights about the equilibrium state of homogeneous turbulence that is sheared in rotating frames. For example, these results suggest that the equilibrium value of the ratio of the production rate to the dissipation rate ( $P/\epsilon$ ) of the turbulent kinetic energy is a function of the ratio of the frame rotation rate to the mean shear rate ( $\Omega^f/S$ ). This is true even for those values of  $\Omega^f/S$  corresponding to the “unstable regime”, where the turbulent kinetic energy,  $k$ , and its dissipation rate,  $\epsilon$ , grow exponentially in time. Here

we have also shown that structure-based turbulence models using the large-scale enstrophy equation are in good agreement with DNS results. This suggests that these models are good candidates for use in turbomachinery CFD codes, and we have initiated work aiming at a simplified two-equation algebraic structure-based model for use in engineering codes. We expect to be able to report our progress in this direction in the short future.

## REFERENCES

- Bardina, J., Ferziger, J. H., and Reynolds, W. C., 1983, “Improved turbulence models based on large eddy simulation of homogeneous, incompressible turbulent flows”, Technical Report TF-19, Dept. Mech. Engineering, Stanford University.
- Kassinis S. C., Reynolds, W. C. and Rogers, M. M., 2001, “One-Point Turbulence Structure Tensors”, *J. Fluid Mech.*, **428**, pp.213-248.
- Kassinis S. C., Langer, C. A., Haire, S., and Reynolds, W. C., 2000, Structure-based modeling for wall-bounded flows. *Int. J. Heat and Fluid Flow*, **21**(5), pp 599-605.
- Kassinis, S. C. and Reynolds, W. C., 1994, “A Structure-Based Model for the Rapid Distortion of Homogeneous Turbulence”, Report TF-61. Mech. Eng. Dept., Stanford University.
- Launder, B. E., Reece G. J., and Rodi, W., 1975, “Progress in the development of a Reynolds stress turbulence closure,” *J. Fluid Mech.*, **68**, p. 537.
- Lumley, J. L., 1978, “Computational modeling of turbulent flows,” *Adv. Appl. Mech.*, **18**, p. 123.
- Poroseva, S. V., Kassinis, S. C., Langer, C. A. and Reynolds, W. C., 2002, “Structure-Based Turbulence Model: Application to a Rotating Pipe Flow”, *Phys. Fluids*, **14**(4), pp. 1523-1532.
- Reynolds, W. C., Langer, C. A., and Kassinis, S. C., 2002, “Structure and Scales in Turbulence Modeling”, *Phys. Fluids*, **14**(7), pp. 2485-2492.
- Reynolds, W. C. and Kassinis, S. C., 1995, “One-Point Modeling of Rapidly Deformed Homogeneous Turbulence”, *Proc. R. Soc. Lond. A*, **451**, pp. 87-104.
- Reynolds, W. C., 1989, “Effects of Rotation on Homogeneous Turbulence”, In *Proc. 10<sup>th</sup> Australasian Fluid Mechanics Conf. (U. Melbourne)*.
- Rogallo, R., 1981, “Numerical Experiments in Homogeneous Turbulence”, NASA Memo 81315.

